V ECCOMAS Thematic Conference on the Mechanical Response of Composites
COMPOSITES 2015
S.R. Hallett and J.J.C. Remmers (Editors)

A thick level set interface model for simulating fatigue-driven delamination in composites

M. Latifi*, **F.P. van der Meer, L.J. Sluys**

Delft University of Technology, Faculty of Civil Engineering and Geosciences,
PO Box 5048, 2600 GA Delft, The Netherlands
*m.latifi@tudelft.nl

Keywords: Composites, Delamination, Fatigue, Thick level set, Interface element.

Summary: *This paper presents a new damage model for simulating fatigue-driven delamination in composite laminates. This model is developed based on the Thick Level Set approach (TLS) and provides a favorable link between damage mechanics and fracture mechanics through the non-local evaluation of the energy release rate. Previously, this approach has been applied in the context of quasi-static continuum damage models. In this work, the thick level set method is translated to an interface model. The new interface damage model can be applied to quasi-static and fatigue simulations. It benefits from the kinematic flexibility of interface elements and preferable use of fracture mechanics for fatigue analysis. A 3D model is developed based on this approach and the obtained numerical results are validated with analytical and experimental data.*

1. INTRODUCTION

The thick level set approach (TLS) to model damage growth in solids was first introduced by Möes et al. [1] in the context of continuum damage model. The model contains a non-local treatment to avoid spurious localizations. This non-local treatment appears when the energy release rate is computed by integrating local values of energy over the width of a transition zone. In this zone, the damage variable is computed as an explicit function of the level set field, and changes between 0 and 1. The computational effort for regularization is done in this transition zone. Bernard et al. [2] improved this model to a robust and easy to implement model with an explicit damage growth algorithm. Van der Meer and Sluys [3] extended this continuum model by introducing a special interphase material and a strength-based initiation parameter for simulating the cusp formation at the core of a sandwich in a shear test. In this paper, using interface elements, a discontinuous damage model for fatigue is presented based on the TLS. The discontinuity is defined at the interface using interface elements.

In the context of fatigue analysis the VCCT has been employed to obtain the energy release rate of a growing crack[4]. This is embedded in the Paris law to compute the crack growth rate under fatigue loading. The application of this approach is limited to the self-similar growth of cracks because for an accurate computation of the energy release rate the mesh must be aligned with the crack front.

An alternative approach for modeling delamination is by using interface elements. The interface elements are a conventional tool for modeling interfacial failure in composites. They are widely used for simulating delamination in composites under quasi-static and fatigue loading. For fatigue analysis, numerical models usually provide a link between fracture mechanics and damage mechanics based on local extraction of the energy release associated with crack growth from the cohesive law. Turon et al. [5] proposed a high-cycle fatigue model based on this approach. However, the local computation of the energy release rate requires an idealization of the cohesive fatigue response and an estimation of the length of cohesive zone, which are both problematic. Harper and Hallett [6] proposed a new formulation based on locally extracting the energy release rate from interface elements. They proposed the division of the cohesive zone into two equal regions: a static damage zone and a fatigue damage zone. The model showed an improvement in approximating the traction-displacement response of interface elements; however, it needs further investigation about the correctness of assumption of having two different regions with equal length in the cohesive zone. Kawashita and Hallett [7] proposed a crack tip tracking algorithm which eliminates the dependency of the cohesive interface model to the length of cohesive zone. This paper proposes an alternative non-local method for extracting the energy release rate from interface elements based on the thick level set approach [1, 2]. In this new discontinuous TLS, the local values of dissipated energy are a function of displacement jumps at the material discontinuity. This is in contrast with the continuum TLS models proposed in [1, 2, 3] where the local energy dissipation was a function of strain. This model benefits from a direct transition between damage and fracture mechanics which is a key point in embedding the Paris law in the formulation of the fatigue model. The model is validated by simulating a double cantilever beam (DCB) test and a circular delamination benchmark.

2. Damage model

In this section we first explain the local governing equations at the material discontinuity and then discuss the method of computing the non-local energy release rate.

2.1 Local governing equations

The constitutive law of interface elements that relates the displacement jump Δ to the traction τ in a material discontinuity is derived from the definition of free energy. The free energy per unit surface of interface is expressed as

$$\varphi(\Delta, d) = (1 - d)\varphi_0(\Delta) \tag{1}$$

where Δ is a vector that contains the displacement jump components in local coordinates and d is a damage parameter which is considered to be a function of level set field (ϕ) which will be introduced in section 2.2 This definition of damage is in contrast with the cohesive zone approach, where the damage is usually considered as a function of displacement jump (Δ). The variable φ_0 in Eq.(1) is defined as

$$\varphi_0(\Delta) = \frac{1}{2}\Delta_i K \delta_{ij} \Delta_j, i = 1, 3; j = 1, 3 \tag{2}$$

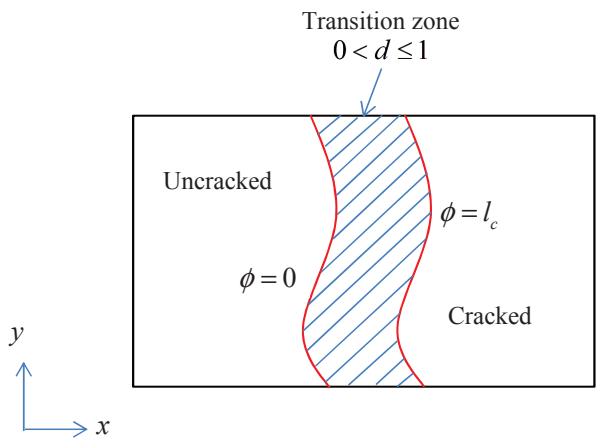

Figure 1. The transition zone between cracked and uncracked material

where K is the dummy stiffness in this equation. This expression for free energy φ is valid for tension dominant cases; however, in compression the negative value of normal displacement jump Δ_3 means interpenetration at the contact surface which does not have any physical meaning. Therefore, to prevent interfacial interpenetration, following Turon et al. [8], Eq.(1) is modified into

$$\varphi(\Delta, d) = (1-d)\varphi_0(\Delta_i) + d\varphi_0(\delta_{3i}\langle -\Delta_3 \rangle) \tag{3}$$

where δ_{ij} is the Kronecker delta and the MacAuley bracket is defined as $\langle x \rangle = \frac{1}{2}(x + |x|)$. The traction-displacement law at the material discontinuity is obtained by differentiation the free energy with respect to the displacement jump:

$$\tau_i = \frac{\partial \varphi}{\partial \Delta_i} = (1-d)K\delta_{ij}\Delta_j - dK\delta_{ij}\delta_{3j}\langle -\Delta_3 \rangle \tag{4}$$

The local driving force for damage growth is obtained by differentiating of the free energy with respect to the damage variable:

$$Y = \frac{\partial \varphi}{\partial d} = -\varphi_0(\Delta_i) + \varphi_0(\delta_{3i}\langle -\Delta_3 \rangle) \tag{5}$$

2.2 Damage definition in the TLS approach

In the TLS method a length scale (l_c) is embedded in the wake of the front which determines the size of the transition zone (see Fig.1). The damage is changing between 0 and 1 in this zone and a level set function [9] defines the crack front location. This level set function is a signed distance function and the value of damage in the zone between cracked and uncracked material is a function of the level set field.

The iso-zero of this function is the damage front. The size of this damage zone (l_c) is equal to the minimum distance between the crack front ($\phi = 0$, $d = 0$), and the point where ($\phi = l_c$, $d = 1$). In this region the damage grows from 0 to 1 as ϕ decreases from 1 to 0.

2.3 Non-local computation of energy release rate

In the TLS approach the energy released due to the growth of a crack is obtained as a non-local quantity by integrating the local driving force over the transition zone. Using the local definition of energy in Eq.(5), the configurational force is defined as

$$G(s) = \int_0^l d'(\phi) Y(\phi, s) d\phi \tag{6}$$

where l_c is the size of the transition band and $d'(\phi)$ is the spatial derivative of damage.

Eq.(6) enables to compute the energy release rate along the damage front; however, to update the level set field the nodal value of dissipated energy needs to be known along the front. Therefore, an average value of the local driving force, $\bar{Y}$ is introduced:

$$G(s) = \int_0^l d'(\phi) \bar{Y}(s) d\phi = \bar{Y}(s) \int_0^l d'(\phi) d\phi = \bar{Y}(s) \tag{7}$$

The field $\bar{Y}$ is discretized over the nodes of elements at the transition band. The constraint that $\bar{Y}$ is constant in ϕ direction ($\nabla \bar{Y}.\nabla \phi = 0$) should be applied. Following Van der Meer et al. [3], the combination of Lagrange multipliers and the Galerkin method is employed which results in the following system of equations:

$$\begin{bmatrix} K & L \\ L & 0 \end{bmatrix} \begin{Bmatrix} \bar{Y} \\ l \end{Bmatrix} = \begin{Bmatrix} f^y \\ 0 \end{Bmatrix} \tag{8}$$

The matrices and the right hand side vectors are defined as

$$K_{ij} = \int_{\Omega^d} d' N_i N_j + \frac{\kappa h^2}{l_c} \frac{\partial N_i}{\partial x_k} \frac{\partial N_j}{\partial x_k} d\Omega \tag{9}$$

$$L_{ij} = \int_{\Omega^d} l_c \left(\frac{\partial N_i}{\partial x_k} \frac{\partial \phi}{\partial x_k} \right) \left(\frac{\partial N_j}{\partial x_k} \frac{\partial \phi}{\partial x_k} \right) d\Omega \tag{10}$$

$$f_i^Y = \int_{\Omega^d} N_i d' Y d\Omega \tag{11}$$

To stabilize the field $\bar{Y}$, a diffusion term is added in Eq.(9), where κ is a stabilization parameter, h is the typical element size, and N is the shape function.

3. Crack growth model

Extracting the energy release rate with system of equations (8) provides the possibility of computing the growth of crack under fatigue loading condition, using the Paris law. The Paris law relates the energy release rate to the crack growth rate:

$$\frac{da}{dN} = C(\beta, R)\left(\frac{\Delta G(R)}{G_c(\beta)}\right)^{m(\beta,R)} \tag{12}$$

where C and m are material constants that depend on the mode ratio and load ratio R, the fracture energy G_c is a function of mode ratio (β), and the load ratio R is considered as the minimum over the maximum cyclic load (P_{min}/P_{max}). In this equation, the cyclic variation of energy release rate ΔG is defined as

$$\Delta G = (1 - R^2)G \tag{13}$$

where the value of G is obtained from solving equation 8.

Computing the crack growth rate from Eq.(12) allows to obtain the front increment:

$$a(s) = \frac{da}{dN}\Delta N \tag{14}$$

where ΔN is the number of skipped cycles based on a cycle jump strategy:

$$\Delta N = \frac{a_{max}}{(\frac{da}{dN})_{max}} \tag{15}$$

where a_{max} is the maximum value of a which is considered smaller than the element size to ensure stability of the explicit level set update, and $(\frac{da}{dN})_{max}$ is the maximum of crack growth rate along the front. The computed front movement in Eq.(14) is extended through the domain and used to update the level set field. The updated level set field defines the new damage distribution in the next time step and this procedure continues until the end of the simulation.

3.1 Mixed mode loading

In order to enable the proposed level set model to deal with mixed-mode loading conditions, the dependence of G_c, m and C on the mode-ratio is defined. The mode ratio effect on the G_c is considered using an expression presented by Benzeggagh and Kenane [10]:

$$G_c = G_{Ic} + (G_{IIc} - G_{Ic})(\beta)^{\eta} \tag{16}$$

where η is a mode interaction parameter, G_{Ic} and G_{IIc} are fracture energy in modes I and II, and the mode ratio β is defined as

$$\beta = \frac{G_{II} + G_{III}}{G} = \frac{G_{shear}}{G} \tag{17}$$

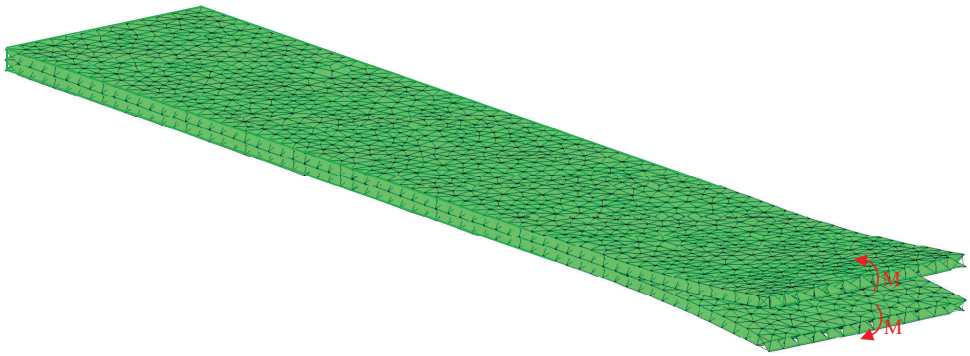

Figure 2. Loading pattern in mode I simulation

where considering Eq.(7) the value of G_{shear} is equal with $\bar{Y}_{shear}$. To obtain the shear contribution of the averaged configurational force ($\bar{Y}_{shear}$), Eq.(8) is solved once more:

$$\begin{bmatrix} K & L \\ L & 0 \end{bmatrix} \begin{Bmatrix} \bar{Y}_{shear} \\ l \end{Bmatrix} = \begin{Bmatrix} f^y \\ 0 \end{Bmatrix} \tag{18}$$

where at the right hand side in Eq.(11), Y_{shear} is used instead of Y.

The dependence of parameters C and m on the mode ratio is introduced accordingly [11]

$$\log C = \log C_I + (\beta) \log C_m + (\beta)^2 \log \frac{C_{II}}{C_m C_I} \tag{19}$$

$$m = m_I + m_m (\beta) + (m_{II} - m_I - m_m)(\beta)^2 \tag{20}$$

where subscripts I, II and m illustrate mode I, mode II, and mixed mode loading conditions for parameters C and m.

4. Results and discussion

Simulations of a mode I delamination test and a circular delamination benchmark were conducted to demonstrate that the model can accurately simulate the response of the test specimens under cyclic loading.

4.1 Simulation of DCB test case

To verify the capability of the proposed fatigue model a 3D finite element model of a double cantilever beam under mode I loading was analyzed. The dimensions and the material properties (see Table 1) of the specimen were the same as in the experimental test case introduced by Asp et al. [12]. The HTA/6376C carbon/epoxy specimen was 150 mm long, 20 mm wide with two 1.55 mm thick arms and a 35 mm pre-crack at the mid-plane of the specimen. In the numerical model one layer of 6-node wedge elements were considered in both arms which were connected with interface elements at the mid-plane of the specimen.

E_{11}	E_{22}=E_{33}	G_{12}=G_{13}	G_{23}
120.0 GPa	10.5 GPa	5.25 GPa	3.48 GPa
$\nu_{12} = \nu_{13}$	ν_{23}	G_{Ic}	G_{IIc}
0.3	0.51	0.260 kJ/m^2	1.002 kJ/m^2

Table 1. Material properties for HTA/6376C [12, 13]

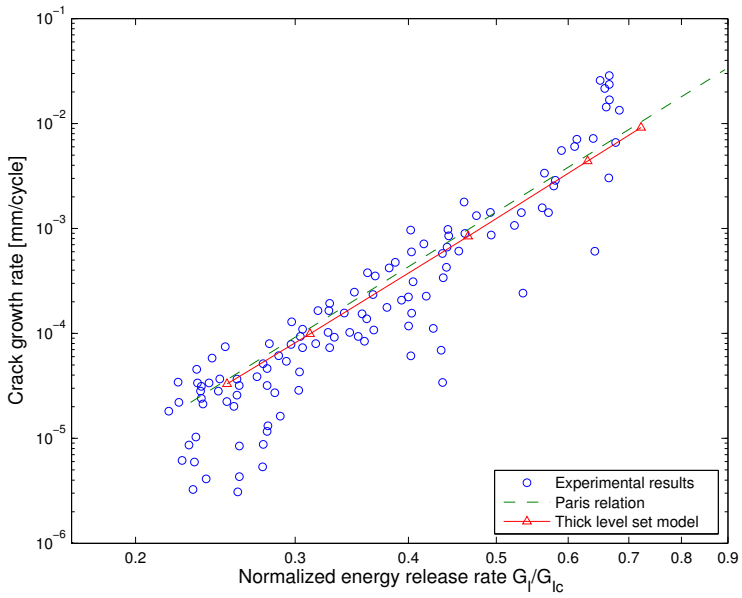

Figure 3. Comparison of crack growth rate obtained from thick level set model with experimental data and theoretical Paris law for DCB tests

In this simulation the characteristic length and the value of lc were 0.89 mm and 5 mm, respectively. Table 2 presents the fatigue material properties of the specimen.

To obtain the constant crack growth rate in a mode I loading simulation two opposing moments were applied at the arms of the specimen (see Fig. 2). The simulation was repeated with different values of applied moments and the computed crack growth rates versus normalized energy release rate are presented in Fig. 3.

C_I(mm/cycle)	C_{II}(mm/cycle)	C_m(mm/cycle)	η
0.0616	2.99	458087	2.73
m_I	m_{II}	m_m	
5.4	4.5	4.94	

Table 2. Fatigue material properties for HTA/6376C [5]

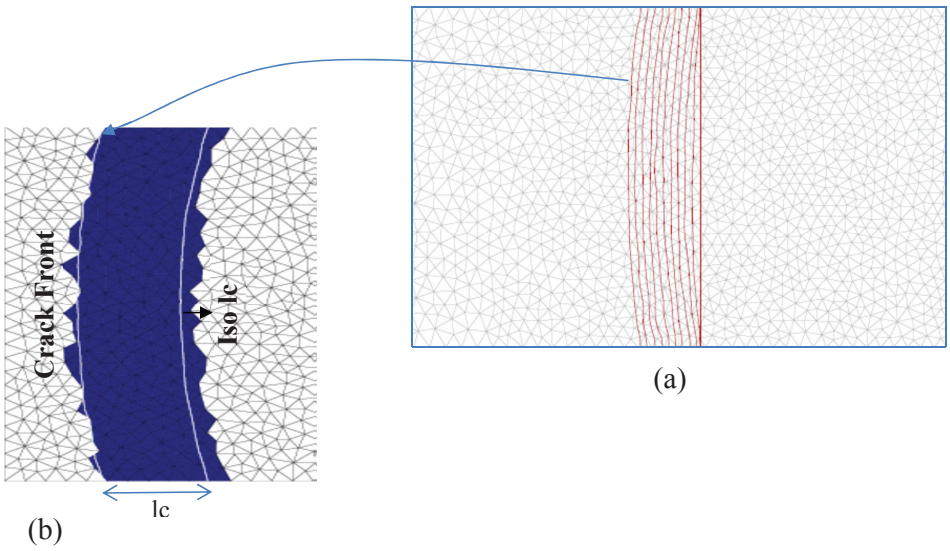

Figure 4. DCB simulation: (a) delamination growth (b) corresponding transition zone with length l_c

The energy release rate used along the horizontal axis in Fig. 3, is obtained from the applied moments using the analytical formula:

$$G_I = \frac{M^2}{bEI} \tag{21}$$

where E is the longitudinal flexural Young's modulus, b is the specimen width, and I is the second moment of area of the specimen's arms. Fig. 3 presents a comparison between the obtained numerical results from the thick level set interface model, the experimental results and direct evaluation of the Paris law. The comparison shows a good agreement between experimental an numerical results. It can be observed that the Paris relation that was implemented locally in the model is retrieved accurately from the results which means that the procedure for the non-local computing of G in the proposed model is accurate. Fig. 4 presents the damage front evaluation and corresponding transition zone with length l_c.

4.2 Circular delamination test

The simulation of delamination propagation at the interface of an isotropic circular plate under mode II loading was performed. The quasi-isotropic properties of this composite plate allows the homogenization of in-plane properties which are introduced in table 3. The radius of the plate was 100 mm with a total thickness of 4 mm and a non-circular pre-crack at the interface of the plate. Considering the symmetry of the plate with homogenized properties, only one quarter of the specimen was simulated. One layer of 6-node wedge elements was considered at two homogenized thin plates which were connected with interface elements. Following the

ν	E(GPa)	G_{IIc}(N/mm)
0.3	60	0.8

Table 3. Isotropic material properties for T800/924 laminate [14]

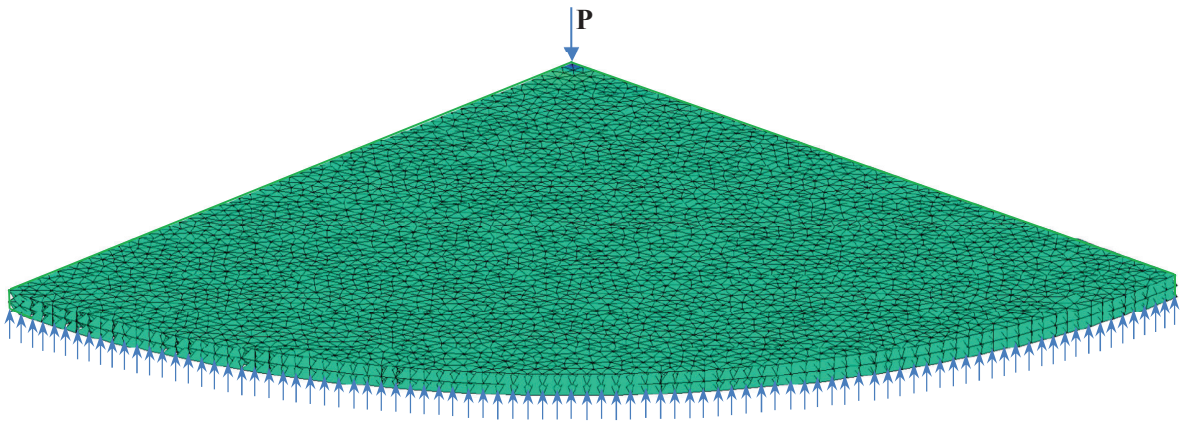

Figure 5. Boundary conditions in the circular delamination simulation

loading envelope approach for fatigue analysis a single load point was applied at the center of the plate (Fig. 5) for an R-ratio of 0.1.

Figure 6 shows crack propagation at the interface of the plate. Delamination started from a non-circular pre-crack and it develops into a circular shape as delamination develops along the interface. This circular growth corresponds to experimental observations in the quasis-static NAFEMS benchmark [14] and fatigue simulation of circular delamination in [7]. Figure 7 shows the front intersection location versus number of elapsed cycles along X and Y axes. The figure illustrates that at the beginning of the delamination process the growth rate is higher in X direction and it becomes equal with the growth rate in Y direction as the crack front tends to the circular shape.

5. Conclusion

In this paper, a thick level set interface model is proposed for simulating fatigue-driven delamination in composites. This 3D model benefits from the kinematic capabilities of interface elements. Furthermore, using the thick level set method provides the possibility of defining the crack front location with a level set function and the non-local extracting of the energy release rate. The non-locality appears by integrating the local values of energy along the defined transition zone based on the thick level set method. In contrast with the previous continuum thick level set models which computes the energy release rate using a strain tensor, in our discontinuous model it is defined as a function of computed displacement jumps in interface elements. The presented fatigue model is able to predict the crack growth rate and the delamination growth pattern accurately. This was proven by simulating a DCB test and comparing the resulting crack

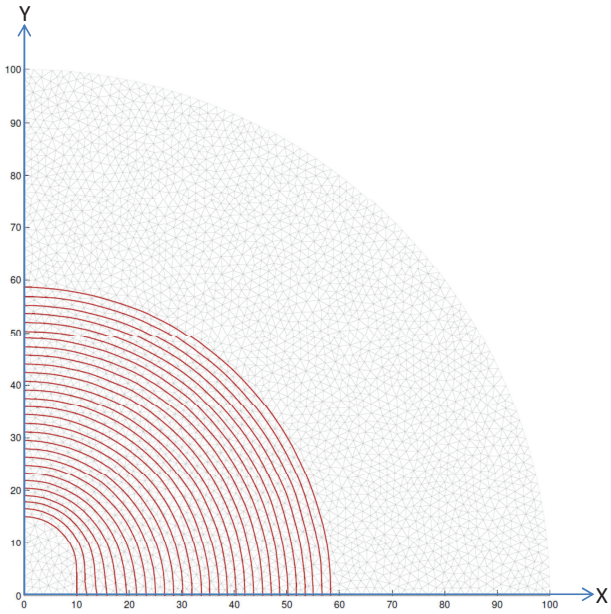

Figure 6. Damage front shape in circular delamination simulation

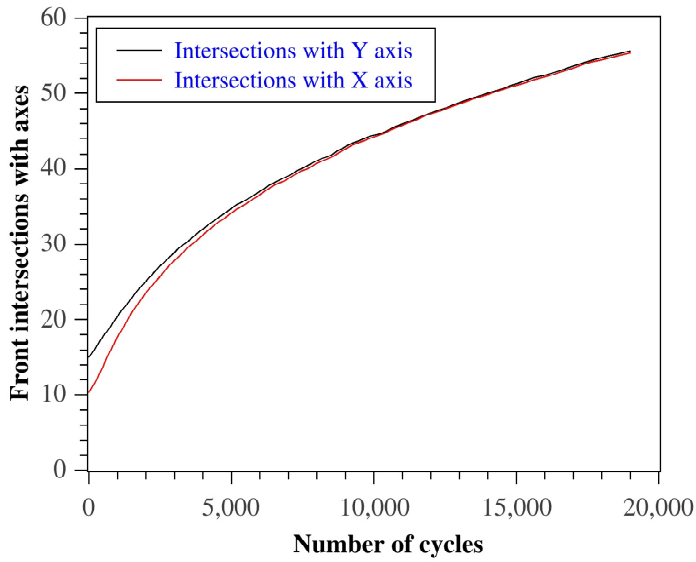

Figure 7. Tip location versus number of cycles

growth rate with experimental data. Furthermore, results from a circular delamination simulation were compared with experimental observations. The resulting crack growth rate from the DCB simulation and the predicted trend of delamination in the circular delamination match well with experimental observations.

References

[1] N. Moës, C. Stolz, P. E. Bernard, and N. Chevaugeon. A level set based model for damage growth: The thick level set approach. *Int. J. Numer. Methods Eng.*, 86(3):358–380, 2011.

[2] P. E. Bernard, N. Moës, and N. Chevaugeon. Damage growth modeling using the Thick Level Set (TLS) approach: Efficient discretization for quasi-static loadings. *Comput. Methods Appl. Mech. Eng.*, 233-236:11–27, 2012.

[3] F. P. van der Meer and L. J. Sluys. The Thick Level Set method : sliding deformations and damage initiation. *Comput. Methods Appl. Mech. Eng.*, 2014.

[4] R. Krueger. Virtual crack closure technique: History, approach, and applications. *Appl. Mech. Rev.*, 57(2):109–143, 2004.

[5] A. Turon, J. Costa, P. P. Camanho, and C. G. Dávila. Simulation of delamination in composites under high-cycle fatigue. *Compos. Part A Appl. Sci. Manuf.*, 38(11):2270–2282, 2007.

[6] P. W. Harper and S. R. Hallett. A fatigue degradation law for cohesive interface elements – Development and application to composite materials. *Int. J. Fatigue*, 32(11):1774–1787, 2010.

[7] L. F. Kawashita and S. R. Hallett. A crack tip tracking algorithm for cohesive interface element analysis of fatigue delamination propagation in composite materials. *Int. J. Solids Struct.*, 49(21):2898–2913, 2012.

[8] A. Turon, P. P. Camanho, J. Costa, and C. G. Dávila. A damage model for the simulation of delamination in advanced composites under variable-mode loading. *Mech. Mater.*, 38(11):1072–1089, 2006.

[9] J. A. Sethian. *Level Set Methods and Fast Marching Methods: Evolving Interfaces in Computational Geometry, Fluid Mechanics, Computer Vision, and Materials Science*. Cambridge University Press, 1999.

[10] M. L. Benzeggagh and M. Kenane. Measurement of mixed-mode delamination fracture toughness of unidirectional glass/epoxy composites with mixed-mode bending apparatus. *Compos. Sci. Technol.*, 56(4):439–449, 1996.

[11] N. Blanco, E. K. Gamstedt, L. E. Asp, and J. Costa. Mixed-mode delamination growth in carbon–fibre composite laminates under cyclic loading. *Int. J. Solids Struct.*, 41(15):4219–4235, 2004.

[12] L. E. Asp, A. Sjögren, and E. S. Greenhalgh. Delamination Growth and Thresholds in a Carbon/Epoxy Composite Under Fatigue Loading. *J. Compos. Technol. Res.*, 23(2):55–68, 2001.

[13] P. Robinson, U. Galvanetto, D. Tumino, G. Bellucci, and D. Violeau. Numerical simulation of fatigue-driven delamination using interface elements. *Int. J. Numer. Methods Eng.*, 63(13):1824–1848, 2005.

[14] G. A. O. Davies. Benchmarks for composite delamination. *NAFEMS Ltd., Hamilton, UK.*, 2002.